ACS Medicinal Chemistry Letters

Letter

Polysaccharide-Based Nanoparticles for Two-Step Responsive Release of Antitumor Drug

Hong-Guang Fu, Yong Chen, Qilin Yu, and Yu Liu

ACS Med. Chem. Lett., **Just Accepted Manuscript** • DOI: 10.1021/acsmedchemlett.0c00040 • Publication Date (Web): 18 May 2020

Just Accepted

is published by the American Chemical Society. 1155 Sixteenth Street N.W., Washington, DC 20036

Polysaccharide-Based Nanoparticles for Two-Step Responsive Release of Antitumor Drug

Hong-Guang Fu, † Yong Chen,† Qilin Yu,† and Yu Liu*†

† College of Chemistry, State Key Laboratory of Elemento-Organic Chemistry, Nankai University, Tianjin 300071, China

ABSTRACT: A novel two-step in situ method for targeted antitumor drug release by supramolecular assembly (Fc-CPT@HACD) was constructed using camptothecin prodrug (Fc-CPT) and β-cyclodextrin (β-CD) modified hyaluronic acid (HACD). Benefitting from the overexpressed H_2O_2 and glutathione (GSH) in tumor cells, Fc-CPT@HACD is able to disassemble by oxidizing ferrocene (Fc) to Fc^+, leading to an efficient release of anti-cancer drug camptothecin (CPT) to induce tumor cells apoptosis with normal cells remaining unaffected. The in vivo experiment results also demonstrated that Fc-CPT@HACD possessed higher anticancer efficiency than free CPT, accompanied by negligible side effects.

KEYWORDS: *Supramolecular assembly • Cyclodextrin • HACD • Multi-stimuli responsive • Tumor targeting*

The construction of novel targeting stimuli-responsive supramolecular drug systems (SDSs) by simple noncovalent interactions has attracted considerable attention to overcome several drawbacks (severe side effects, nonspecific distribution, systemic instability, rapid blood clearance, etc.)[1-2] of conventional chemotherapeutic agents by achieving controlled drug release. These stimuli includes internal features (redox potential,[3] hypoxic microenvironment,[4] glucose level,[5] enzymatic activity,[6] reduced pH,[7] ATP level,[8] etc.) and external triggers (temperature,[9] light,[10]ultrasound,[11] magnetic field,[12] etc.). As majorities of noncovalent interactions are easily destroyed in internal environment before they reached the nidus, possibly causing side effects, the resultant SDSs need to be protected thoughtfully. Hydrophobic interactions based macrocyclic host-guest stimuli-responsive supramolecular assemblies have been developed and opened the prospect of cancer therapy both in vitro and in vivo.[13-14] One particular macrocycle, β-cyclodextrin (β-CD, composed by seven D-glucopyranose units), is distinguished by its significant controlled capture and release behavior between β-cyclodextrin and ferrocene in aqueous solution.[15] Moreover, most of the cyclodextrin derivatives showed good water solubility, negligible toxicity in animals, excellent biocompatibility further promoting their biomedical applications.[16] On the other hand, by trapping free radicals, abnormal GSH serves as an antioxidant to control the oxidative stress in redox homeostasis. As the concentration of GSH in tumor cells (~ 10 mM)[17] is hundreds of times higher than that in normal cells, the disulfide bonds that are cleavable by GSH have been greatly studied as redox responsive linkers in supramolecular assemblies with specific drug release inside cells.

However, despite great efforts that have been made, most of the existing supramolecular assemblies are not specifically loaded for tumor cells. Recently, introducing malignant tumors targeting ligands (such as folic acid,[18] biotin,[19] transferrin,[20] sugars[21]) on assemblies to enhance the drug accumulation in cancer tissues accompanying insignificant toxicity to normal tissues becomes an popular strategy to overcome this problem. Besides the above mentioned targeting ligands, hyaluronic acid (HA), a biocompatible, biodegradable and water-soluble polysaccharide was also used extensively.[22-24]

In the present work, taking advantage of the host-guest binding affinity between β-CD and ferrocene,[25] supramolecular assembly (Fc-CPT@HACD) with hydrophilic HA shell (Scheme 1), which may protect CPT prodrug from hydrolysis against water, was constructed. To our delight, the supramolecular assembly shows an excellent targeting ability towards tumor cells and issues, negligible cytotoxicity to normal issues, effective drug release both in vitro and in vivo. After Fc-CPT@HACD get into tumor cells, the intrinsically higher H_2O_2 in the cytoplasm would oxidize Fc to Fc^+ and further destroy the binding activity between Fc and β-CD. Without the protection of HA shells, the exposed disulfide bonds that linking CPT and Fc are cut off[26] resulting in a fast release of CPT eventually make it a promising candidate for selective inhibition of tumor growth.

Scheme 1. Construction of the supramolecular assembly Fc-CPT@HACD and its application for H_2O_2

and GSH triggered release of CPT through intravenous injection.

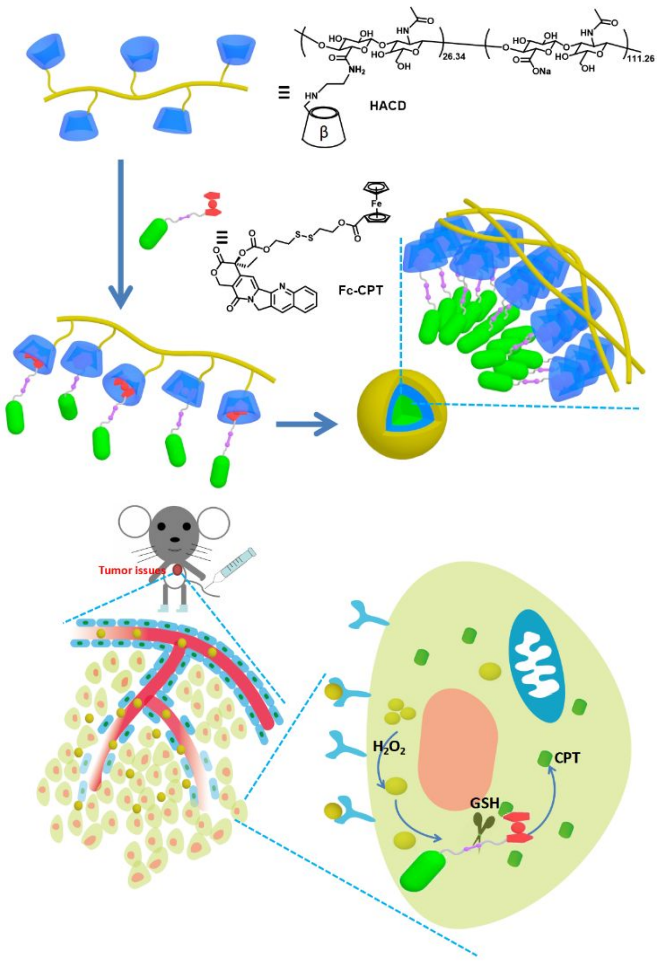

With the excellent host and guest in hand, the binding properties were studied. As β-CDs in HACD provide many binding sites, native β-CD (99% purity) was employed as a model host to investigate the supramolecular interactions between Fc-CPT and β-CD by UV-vis titration in PBS (0.01 M) containing 5% DMSO (99.8% purity). As shown in Fig. 1a, the Job's plot indicated a 1:1 stoichiometry between β-CD and Fc-CPT, in which the minimum spot appeared at 0.5. With the gradual addition of β-CD, the characteristic UV absorbance of Fc-CPT decreased dramatically in the range from 245–404 nm (Fig. 1b) accompanied by a slight red shift, suggesting a conversion from free Fc-CPT to a host-guest specie Fc-CPT@β-CD. Fortunately, the 2D ROESY showed obvious NOE which was in accordance with UV titration result (Fig. S2). Moreover, the binding constant between Fc-CPT and β-CD was determined to be $(1.5 \pm 0.5) \times 10^3$ M^{-1} by nonlinear least-squares fit of the UV titration data at 261 nm (Fig. S3), which is comparable to the reported Ks between Fc-CPT and β-CD.[21]

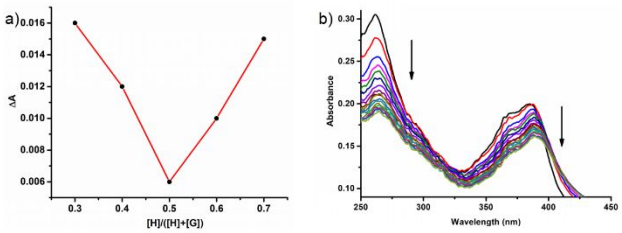

Figure 1. a) Job's plot for Fc-CPT upon complexation with β-CD in pH = 7.2 PBS containing 5% DMSO. b) UV-vis spectra of Fc-CPT (1.0×10^{-5} M) upon addition of native β-CD in pH = 7.2 PBS containing 5% DMSO.

Dynamic light scattering (DLS), scanning electron microscope (SEM), high-resolution transmission electron microscopy (HR-TEM), Tyndall effect and zeta potential experiments were used to investigate the size, morphology and surface charge of Fc-CPT@HACD ([Fc-CPT] = 0.01 mM). The critical aggregation concentration (CAC) of the Fc-CPT@HACD was investigated by monitoring the dependence of the optical transmittance at 260 nm on the concentration of Fc-CPT (Fig. S4), and the CAC value was measured as 2.97×10^{-3} mM. The host molecule HACD could form fiber-like aggregates with a length of several micrometers (Fig. S5). Upon addition of Fc-CPT, the fiber-like aggregates converted to spherical particles. This implied that the Fc-CPT@HACD system existed in forms of aggregation, which was also certificated by the Tyndall effect (Fig. 2d). TEM images showed the morphology of Fc-CPT@HACD as discrete nanoparticles with an average diameter of 50–76 nm (Fig. 2a) by counting about 100 particles. Moreover, the hydrodynamic diameter (Dh) of Fc-CPT@HACD was measured as ca. 63 nm by DLS with a narrow distribution (Fig. 2b), which was consistent with the diameter obtained by TEM. The zeta potential of HACD and Fc-CPT@HACD were measured as ca. -60.1 mV and -58.1 mV (Fig. 2c and Fig. S6). In addition, the UV-vis spectroscopy of Fc-CPT@HACD was nearly unchanged in fetal bovine serum within 7h (Fig. S7), indicating the structure of Fc-CPT@HACD was greatly maintained. The Fc-CPT loading efficiency (weight of loaded Fc-CPT/weight of feeding drug) and Fc-CPT encapsulation ratio were calculated to be 94.7% and 6.5%, respectively (detailed calculation process was presented in ESI, Fig. S8).

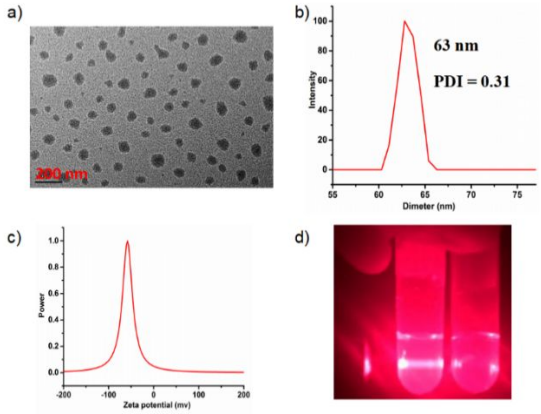

Figure 2. Typical (a) TEM images, (b) DLS, (c) zeta potential of obtained Fc-CPT@HACD (Y axis represented the normalized current intensity) and (d) Tyndall effect of Fc-CPT in the absence (right) and presence (left) of HACD in PBS (pH = 7.2, I = 0.01 M, [Fc-CPT] = 0.01 mM, PBS was made up from Na_2HPO_4 and KH_2PO_4).

Next, the multi-stimuli responsiveness of Fc-CPT@HACD was investigated. It is well known that Fc could be oxidized to Fc^+ by H_2O_2. In the absence of H_2O_2 and GSH, Fc-CPT showed stronger absorption intensity than Fc-CPT@HACD with a slight blue shift. Upon addition H_2O_2 (AR, 30 wt. % in H_2O) or GSH (98% purity), these two UV-vis spectra became similar to each other (Fig. S9, S10) at the end, which could be explained by transition from Fc-CPT to Fc^+-CPT (Fig. S9) or the release of CPT (Fig. S10), which further resulted in the disassembly of the nanoparticles. Moreover, cyclic voltammetry (CV) was used to characterize the electrochemical behaviors of Fc-CPT@HACD and Fc-CPT@HACD + H_2O_2. Fc-CPT@HACD only showed reversible oxidation process, but Fc-CPT@HACD + H_2O_2 showed irreversible oxidation and reduction processes (Fig. S11). The different oxidation potential of Fc-CPT@HACD and Fc-CPT@HACD + H_2O_2 could attribute to the transition from Fc-CPT@HACD to Fc^+-CPT and HACD. Compared with Fig. S7, it was found that Fc-CPT could be released from the Fc-CPT@HACD system in the presence of H_2O_2 in 10 h (Fig. S12). Interestingly, the fluorescence of Fc-CPT@HACD was activated by adding GSH. Upon excitation at 250 nm, the fluorescence of Fc-CPT@HACD + GSH at 450 nm showed a 10-fold enhancement, which was similar to single CPT (Fig. S13). High performance liquid chromatography (HPLC) was also performed to verify the cleavage of CPT from Fc-CPT@HACD upon addition of GSH. As shown in Fig. S14, a peak at 3.5 min (retention time) corresponding to CPT was detected after incubating the supramolecular assembly with GSH.

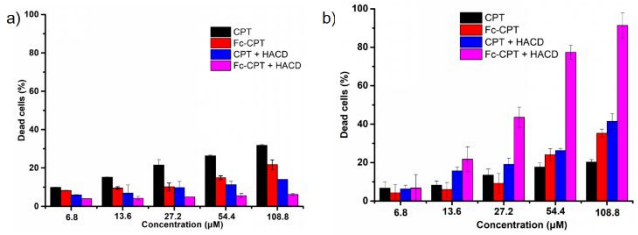

Figure 3. Cellular viability of a) 293T normal cells, b) A549 tumor cells after the treatment with the CPT, Fc-CPT, CPT + HACD and supramolecular assembly Fc-CPT@HACD at various concentrations after incubation 24 h.

The in vitro anticancer efficacy of CPT (98% purity), Fc-CPT, CPT + HACD and supramolecular assembly Fc-CPT@HACD was examined in human lung adenocarcinoma cells (A549 cells, obtained from the cell Center of Peking Union Medical College) and human normal embryonic kidney cells (293T cells, obtained from the cell Center of Peking Union Medical College) by MTT assays. Fig. 3 and Table S1 demonstrated that all of four groups exhibited dose-dependent antitumor activity towards tumor cells and low cytotoxicity toward normal cells. Fc-CPT@HACD even at high concentration of 108.8 μM had no obvious toxicity to 293T cells after incubation for 48 h, indicating the good biocompatibility of the supramolecular assembly. To our delight, even at the concentration of 108.8 μM, separate CPT, Fc-CPT and the mixture of CPT and HACD exhibited no obvious toxicity to A549 cells. The tumor cells mortality was less than 50%, showing a low toxicity to tumor cells, due to their low solubility and weak host–guest binding ability in PBS. In contrast, the supramolecular assembly Fc-CPT@HACD showed more intense cytotoxicity. A relative cellular apoptosis rate of 80% or 95% was observed at 54.4 μM or 108.8 μM. Moreover, the tumor cellular uptake of the supramolecular assembly was investigated by fluorescence confocal microscopy. As shown in Fig. S15, A549 cells displayed a bright blue fluorescence of Fc-CPT in the cytoplasm. We may conclude that the HA moiety of Fc-CPT@HACD specifically recognizes A549 cells by strongly binding to HA receptors on the cell surface, and then it enters the tumor cells through receptor-mediated endocytosis, which further encouraged us to investigate its efficiency in vivo anticancer therapy on A549 tumor implanted mice.

As could be found out in Fig. S16a, there was no significant fluctuation in body weight, suggesting negligible side effects of Fc-CPT@HACD for cancer therapy. Tumor volumes in the mice of the PBS groups were twice as large as it used to be, indicating no inhibition of tumor growth. Positive control groups, free CPT displayed moderate inhibition efficiency, because the drug can hardly reached to tumor tissues. For the mice injected with Fc-CPT@HACD from tail vein, 50% tumor reduction were observed resulting from the higher antitumor efficacy of the supramolecular assembly (Fig. S16b). Compared to the control group for PBS and positive control group for CPT, the tumor growth was about 8.5-fold and 5.4-fold inhibition in the treatment group, respectively, indicating the promises of the Fc-CPT@HACD complex as an anticancer drug. The promising results may attributed to an accumulation of Fc-CPT@HACD in tumor tissues through enhanced permeability and retention effect (EPR effect) and the slow drug releasing performances. Finally, hematoxylin and eosin (H&E) analysis of tumor issues and other major organs (spleen, liver, kidney and lung) were conducted to assess the anti-tumor activity of Fc-CPT@HACD at cellular level (Fig. 4). Clearly, there was no noticeable injury in other organs of the mice. Tumor cells in PBS group showed densest and regular morphology indicating least necrosis. The other control and Fc-CPT@HACD groups showed moderate necrosis and most necrosis. On the basis of these results, we may draw the conclusion

that the targeting Fc-CPT@HACD possessed enhanced antitumor efficiency with slighter side effects than commercially available CPT and was more effective than some systems lacking targeting groups[27-28], lacking stimulus responsiveness[29]or simply loading antitumor drugs through π-stacking[30-31].

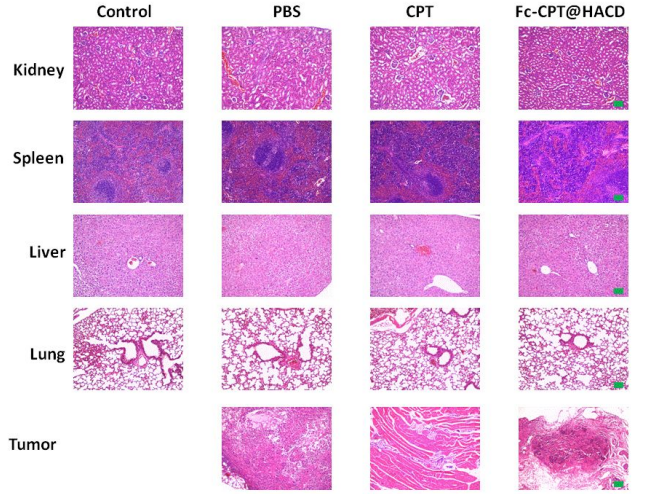

Figure 4. H&E staining of major organs (spleen, liver, kidney and lung) and tumor sections in different treatment groups and the healthy mice as control. Scale bars are 80 μm.

In summary, we developed a stimuli-responsive tumor targeting-specific supramolecular assembly with Fc-CPT and HACD. Benefiting from the overexpressed HA receptor in malignant tumor, the obtained Fc-CPT@HACD could anchor to tumor issues specifically. We further demonstrated that the assembly could respond to H_2O_2 and GSH but with a significantly stability in fetal bovine serum. The overexpressed H_2O_2 in tumor cells could oxide Fc to Fc^+ further causing the disruption of the assembly. Then, the S–S bond was cut off by abundant GSH accompanying the generation of CPT. In vitro and in vivo experiments demonstrated that CPT@HACD possessed higher antitumor efficiency with negligible side affects than PBS and CPT. Thus, we believe that this study will provide a reference to develop a new kind of targeting efficient in situ antitumor drug used in clinic.

ASSOCIATED CONTENT

Supporting Information

The Supporting Information is available free of charge on the ACS Publications website.
Experimental methods and procedures, additional spectra, original data.

AUTHOR INFORMATION

Corresponding Author

* E-mail: yuliu@nankai.edu.cn

Funding Sources

We thank NNSFC (No. 21672113, 21772099, 21971127 and 21861132001) for financial support.

Notes

The authors declare no competing financial interest.

ABBREVIATIONS

GSH, glutathione; CPT, camptothecin; β-CD, β-cyclodextrin; Fc, ferrocene; Fc^+, Ferrocene oxide; HA, hyaluronic acid; A549 cells, human lung adenocarcinoma cells; 293T cells, human normal embryonic kidney cells; EPR effect, enhanced permeability and retention effect. DMSO, dimethyl sulfoxide; CV, cyclic voltammetry.

REFERENCES

(1) Lim, E. K.; Kim, T.; Paik, S.; Haam, S.; Huh, Y. M.; Lee, K., Nanomaterials for theranostics: recent advances and future challenges. *Chem Rev*, **2015**, *115*, 327-394.
(2) Zhou, J.; Yu, G.; Huang, F., Supramolecular chemotherapy based on host–guest molecular recognition: a novel strategy in the battle against cancer with a bright future. *Chem. Soc. Rev.*, **2017**, *46*, 7021-7053.
(3) Kang, Y.; Ju, X.; Ding, L. S.; Zhang, S.; Li, B. J., Reactive oxygen species and glutathione dual redox-responsive supramolecular assemblies with controllable release capability. *ACS Appl. Mater. Interfaces*, **2017**, *9*, 4475-4484.
(4) Feng, L.; Cheng, L.; Dong, Z.; Tao, D.; Barnhart, T. E.; Cai, W.; Chen, M.; Liu, Z., Theranostic liposomes with hypoxia-activated prodrug to effectively destruct hypoxic tumors post-photodynamic therapy. *ACS Nano*, **2017**, *11*, 927-937.
(5) Zhang, Y. M.; Xu, X.; Yu, Q.; Liu, Y. H.; Zhang, Y. H.; Chen, L. X.; Liu, Y., Reversing the cytotoxicity of bile acids by supramolecular encapsulation. *J. Med. Chem.*, **2017**, *60*, 3266-3274.
(6) Such, G. K.; Yan, Y.; Johnston, A. P.; Gunawan, S. T.; Caruso, F., Interfacing materials science and biology for drug carrier design. *Adv. Mater.*, **2015**, *27*, 2278-2297.
(7) Chen, X. M.; Chen, Y.; Hou, X. F.; Wu, X.; Gu, B. H.; Liu, Y., Sulfonato-β-Cyclodextrin mediated supramolecular nanoparticle for controlled release of berberine. *ACS Appl. Mater. Interfaces*, **2018**, *10*, 24987-24992.
(8) Gao, J.; Li, J.; Geng, W. C.; Chen, F. Y.; Duan, X.; Zheng, Z.; Ding, D.; Guo, D. S., Biomarker displacement activation: a general host–guest strategy for targeted phototheranostics in vivo. *J. Am. Chem. Soc.*, **2018**, *140*, 4945-4953.
(9) Hoare, T.; Santamaria, J.; Goya, G. F.; Irusta, S.; Lin, D.; Lau, S.; Padera, R.; Langer, R.; Kohane, D. S., A magnetically triggered composite membrane for on-demand drug delivery. *Nano Lett.*, **2009**, *9*, 3651-3657.
(10) Zhang, Y. M.; Zhang, N. Y.; Xiao, K.; Yu, Q.; Liu, Y., Photo - controlled reversible microtubule assembly mediated by paclitaxel - modified cyclodextrin. *Angew. Chem. Int. Ed. Engl.*, **2018**, *57*, 8649-8653.

(11) Wang, Y.; Shim, M. S.; Levinson, N. S.; Sung, H. W.; Xia, Y., Stimuli-responsive materials for controlled release of theranostic agents. *Adv. Funct. Mater.*, **2014**, *24*, 4206-4220.
(12) Yu, Q.; Zhang, Y. M.; Liu, Y. H.; Liu, Y., Magnetic supramolecular nanofibers of gold nanorods for photothermal therapy. *Adv. Therapeutics*, **2018**, *2*, 1800137.
(13) Wang, X.-Q.; Lei, Q.; Zhu, J.-Y.; Wang, W.-J.; Cheng, Q.; Gao, F.; Sun, Y.-X.; Zhang, X.-Z., Cucurbit[8]uril regulated activatable supramolecular photosensitizer for targeted cancer imaging and photodynamic therapy. *ACS Appl. Mater. Interfaces*, **2016**, *8*, 22892-22899.
(14) Zuo, M.; Qian, W.; Xu, Z.; Shao, W.; Hu, X. Y.; Zhang, D.; Jiang, J.; Sun, X.; Wang, L., Insulin delivery platforms: multiresponsive supramolecular theranostic nanoplatform based on pillar[5]arene and diphenylboronic acid derivatives for integrated glucose sensing and insulin delivery. *Small*, **2018**, *14*, e1801942.
(15) Gong, G.; Cao, Y.; Qian, H.; Zhou, Y.; Zhao, H.; Li, L.; Wang, F.; Zhao, G., Assessment of the antitumor activity of a cyclopalladated ferrocene compound assisted by a dual-targeting drug delivery system. *Chem. Commun.*, **2018**, *54*, 8312-8315.
(16) Yu, G.; Jie, K.; Huang, F., Supramolecular amphiphiles based on host–guest molecular recognition motifs. *Chem. Rev.*, **2015**, *115*, 7240-7303.
(17) Jia, X.; Zhang, Y.; Zou, Y.; Wang, Y.; Niu, D.; He, Q.; Huang, Z.; Zhu, W.; Tian, H.; Shi, J.; Li, Y., Dual intratumoral redox/enzyme responsive NO-releasing nanomedicine for the specific, high-efficacy, and low toxic cancer therapy. *Adv. Mater.*, **2018**, *30*, e1704490.
(18) Chen, C.; Ke, J.; Zhou, X. E.; Yi, W.; Brunzelle, J. S.; Li, J.; Yong, E. L.; Xu, H. E.; Melcher, K., Structural basis for molecular recognition of folic acid by folate receptors. *Nature*, **2013**, *500*, 486-489.
(19) Wang, Y.-X.; Zhang, Y.-M.; Wang, Y.-L.; Liu, Y., Multifunctional vehicle of amphiphilic calix[4]arene mediated by liposome. *Chem. Mater.*, **2015**, *27*, 2848-2854.
(20) Fu, H. G.; Chen, Y.; Yu, Q.; Liu, Y., A tumor-targeting Ru/polysaccharide/protein supramolecular assembly with high photodynamic therapy ability. *Chem. Commun.*, **2019**, 55, 3148-3151.
(21) Zhang, J.; Ma, W.; He, X. P.; Tian, H., Taking orders from light: photo-switchable working/inactive smart surfaces for protein and cell adhesion. *ACS Appl. Mater. Interfaces*, **2017**, *9*, 8498-8507.
(22) Peer, D.; Margalit, R, Tumor-targeted hyaluronan nanoliposomes increase the antitumor activity of liposomal doxorubicin in syngeneic and human xenograft mouse tumor models. *Neoplasia*, **2004**, *6*, 343-353.
(23) Zhang, Y.-H.; Zhang, Y.-M.; Yu, J.; Wang, J.; Liu, Y., Boronate-crosslinked polysaccharide conjugates for pH-responsive and targeted drug delivery. *Chem. Commun.,* **2019**, 55, 1164-1167.
(24) Wu, X.; Chen, Y.; Yu, Q.; Li, F. Q.; Liu, Y., A cucurbituril/polysaccharide/carbazole ternary supramolecular assembly for targeted cell imaging. *Chem. Commun.,* **2019**, 55, 4343-4346.
(25) Rekharsky, M. V.; Inoue, Y., Complexation thermodynamics of cyclodextrins. *Chem. Rev.*, **1998**, *98*, 1875-1918.
(26) Hayashi, K.; Maruhashi, T.; Nakamura, M.; Sakamoto, W.; Yogo, T., One-pot synthesis of dual stimulus-responsive degradable hollow hybrid nanoparticles for image-guided trimodal therapy. *Adv. Funct. Mater.*, **2016**, *26*, 8613-8622.
(27) Cheng, Q.; Yin, H.; Sun, C.; Yue, L.; Ding, Y.; Dehaen, W.; Wang, R., Glutathione-responsive homodithiacalix[4]arene-based nanoparticles for selective intracellular drug delivery. *Chem. Commun.,* **2018,** *54*, 8128-8131.
(28)Sun, G.; He, Z.; Hao, M.; Zuo, M.; Xu, Z.; Hu, X.-Y.; Zhu, J.-J.; Wang, L., Dual acid-responsive bola-type supramolecular vesicles for efficient intracellular anticancer drug delivery. *J. Mater. Chem. B.,* **2019,** *7*, 3944-3949.
(29) Sun, C.; Zhang, H.; Yue, L.; Li, S.; Cheng, Q.; Wang, R., Facile Preparation of Cucurbit[6]uril-Based Polymer Nanocapsules for Targeted Photodynamic Therapy. *ACS Appl. Mater. Interfaces,* **2019,** *11*, 22925-22931.
(30)Liu, J.-H.; Wu, X.; Zhang, Y.-M.; Liu, Y., Photocleavable Supramolecular Polysaccharide Nanoparticles for Targeted Drug Release in Cancer Cells. *Asian J. Org. Chem.,* **2018,** *7*, 2444-2447.
(31) Zhang, Y. M.; Cao, Y.; Yang, Y.; Chen, J. T.; Liu, Y., A small-sized graphene oxide supramolecular assembly for targeted delivery of camptothecin. *Chem. Commun.,* **2014,** 50, 13066-13069.

Insert Table of Contents artwork here